Space Weather and Deep-Space Communications

R. Woo[1]

While Pioneer 11 and Galileo are two missions that experienced radio communication disruptions due to space weather, the success of a mission like Solar Probe, whose goal is to fly by the Sun within a few solar radii of its surface, may depend critically on space weather. It is, therefore, crucial to thoroughly understand how space weather affects radio communications and to identify ways to predict it. In this study, we explain how enhanced small-scale density variations in the corona and solar wind represent space weather to radio communications, because they give rise to enhancements in radio-propagation phenomena such as spectral broadening and fluctuations in intensity and Doppler known as scintillation. Recent advances have been made in understanding enhanced small-scale density variations and their relationship to the Sun, and we show how this makes it possible to use daily observations of unprecedented solar missions like the Solar and Heliospheric Observatory (SOHO) to diagnose, monitor, and forecast adverse space weather for deep-space communications.

I. Introduction

To compensate for the low telemetry rates resulting from the loss of the Galileo high-gain antenna, maintaining a continuous flow of data became a high priority for the Galileo Mission. Thus, when radio communication with the Galileo spacecraft was unexpectedly disrupted on February 7, 1997, the Project anxiously checked out both the spacecraft radio transmitting system and the tracking equipment at the ground stations of the NASA/JPL Deep Space Network (DSN). The problem was traced to neither a ground station nor a spacecraft radio-system failure, but surprisingly to adverse radio-propagation effects caused by space weather. As a result of its interaction with the intervening solar wind plasma, the S-band 2.4-GHz (13-cm) Galileo monochromatic radio signal broadened, and both its intensity and Doppler fluctuated rapidly. The latter fluctuations are known as scintillation. Stars twinkle because of the same intensity scintillation phenomenon produced by light-wave scattering from turbulence in the Earth's atmosphere. Spectral broadening [1] and Faraday rotation [2] of spacecraft radio signals are two of the earliest propagation effects produced by the corona and observed by the DSN.

The inability of the narrowband radio receivers of the NASA ground stations to track the noisy and broadened radio signal led directly to the interruption in Galileo communications and loss of its telemetry. Space weather is a menace to all interplanetary missions, especially when their radio paths pass close to the Sun (small solar elongation ε; see Fig. 1), where the effects are greatest. When Pioneer 11
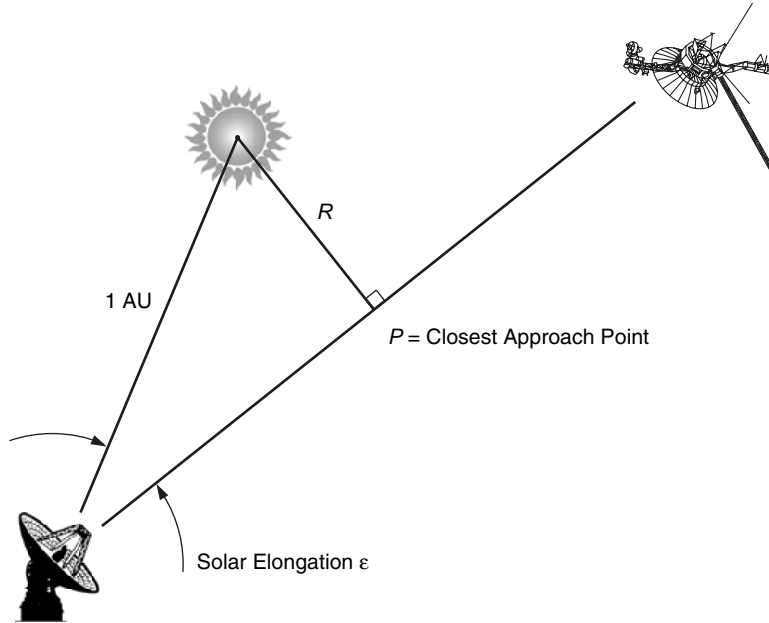
Fig. 1. Geometry of radio occultation measurements of the solar corona. The path-integrated measurements probe the closest approach point P in the corona at a heliocentric distance of R because of the rapid radial falloff in solar wind properties along the radio path. The closest approach point is also defined by the solar elongation ε.

made the first flyby of Saturn in 1979, it was near superior conjunction, and its data rate had to be reduced because of degradation in its radio link due to space weather [3]. For a mission that will one day fly to within a few solar radii of the Sun's surface, such as Solar Probe, space weather effects can be catastrophic. Unlike Galileo and Pioneer 11, for which telemetry retransmission was possible, the Solar Probe encounter data could be lost if the spacecraft fails to survive its close encounter with the unpredictable Sun. Another mission that has space-weather concerns is MESSENGER (Mercury Surface, Space Environment, Geochemistry, and Ranging).[2] As an orbiter around Mercury, Messenger's radio path is always within a solar elongation of 28 deg, making its X-band 8.4-GHz (3.6-cm) (X-band) radio link particularly vulnerable.

While the solar-wind plasma may wreak havoc with space communications, observations of the result-ing radio-propagation phenomena serve as a powerful remote sensing tool for investigating the near-Sun solar wind not yet explored directly by spacecraft. Since the radio source, either natural or man-made and onboard a spacecraft, is occulted by the corona during these observations, we refer to them collectively as radio occultation measurements. Starting with observations of angular broadening by interferometers in the 1950s [4–6], systematic and steady progress has been made toward realizing the full potential of these unique measurements, resulting in the emergence of a deeper understanding of the inferred small-scale coronal variations and their relationship to the Sun and the heliosphere (see, e.g., [7,8] and references therein). These results have also served as a catalyst for unifying disparate observations of the solar wind, the corona, and the Sun, and have improved in significant ways our understanding of the origin and evolution of the solar wind, as well as the coronal magnetic field topology and its influence on solar-wind properties (see, e.g., [9–11] and references therein).

---

[2] http://messenger.jhuapl.edu/

These recent advances, combined with the availability of space missions that continuously monitor the Sun and its atmosphere, e.g., the Solar and Heliospheric Observatory (SOHO)[3] and the recently launched Solar Terrestrial Relations Observatory (STEREO),[4] provide significant practical benefits to the space-weather communication problem. The purpose here is to explain and summarize the highlights relevant to the following key questions: Why and how does space weather disrupt space communications? Since the source of space weather is the Sun, how can available solar observations help diagnose it? How can they be used to monitor and forecast the adverse space weather during the course of DSN tracking?

II. Nature of Space Weather that Impacts Radio Links

Theoretical wave propagation studies have shown that spectral broadening [12]; intensity scintillation, also known as interplanetary scintillation (IPS) [13]; and Doppler (or integrated phase) scintillation [14–17] are radio-propagation phenomena caused by small-scale density fluctuations in the solar wind. Therefore, the systematic increases in spectral broadening and Doppler scintillation with decreasing solar elongation [18–20] evident in Fig. 2 reflect the corresponding systematic increase in the background small-scale density fluctuations toward the Sun. Unlike the spectral broadening and Doppler scintillation in Fig. 2, intensity scintillation saturates near the Sun when strong, i.e., the intensity scintillation relative to its mean approaches unity for all density fluctuations exceeding a critical level [21,22].

As seen in Fig. 2, reproduced from [18], Doppler scintillation varies approximately as $R^{-1.5}$ beyond about $10R_o(\varepsilon \sim 2.7$ deg), which corresponds to an R^{-2} falloff in density fluctuations. Closer to the Sun, the radial falloff is steeper. Since the solar wind expands radially from the Sun and the density fluctuations are proportional to density [7,9], the solar elongation beyond which the density fluctuations fall off as R^{-2} is where acceleration of the solar wind is essentially over, whereas the steeper density falloff closer to the Sun is a manifestation of the acceleration of the solar wind [11].

Space weather produces transients or conspicuous enhancements to this background radial variation or "space climate," as synoptic studies of Doppler scintillation have shown [23]. The key to understanding and forecasting space weather that impacts radio links, therefore, lies in identifying those interplanetary disturbances characterized by enhanced small-scale density fluctuations that produce the scintillation transients and in learning how they are related to the Sun. This has not been straightforward because the small-scale density fluctuations that affect wave propagation are too small to be detected in images of the Sun or the corona. However, enhanced density fluctuations have been shown to be associated with three large-scale features that appear in coronal imaging, and these are described in the following sections.

III. Coronal Mass Ejections

The most prominent propagating large-scale interplanetary disturbance in coronal imaging is the coronal mass ejection (CME), which, if traveling fast enough, also gives rise to a leading interplanetary shock [24–28]. Enhanced small-scale density fluctuations are found within the mass ejection, presumably reflecting the fine structure of its source in the corona (e.g., see Fig. 5 of [29]), and in the compressed plasma ahead of it. Evidence for these enhanced fluctuations comes from radio occultation measurements of interplanetary shocks [30,31], their relationship to in situ solar-wind measurements [32], the close association between scintillation transients and white-light coronal mass ejections [33,34], and in situ measurements of the density fluctuations of coronal mass ejections [35].

Figure 3 shows the time series of the root-mean-square (rms) Doppler scintillation observed by Galileo during 1997 and computed every 3 minutes based on a sampling rate of 1/10 s. Two transients of
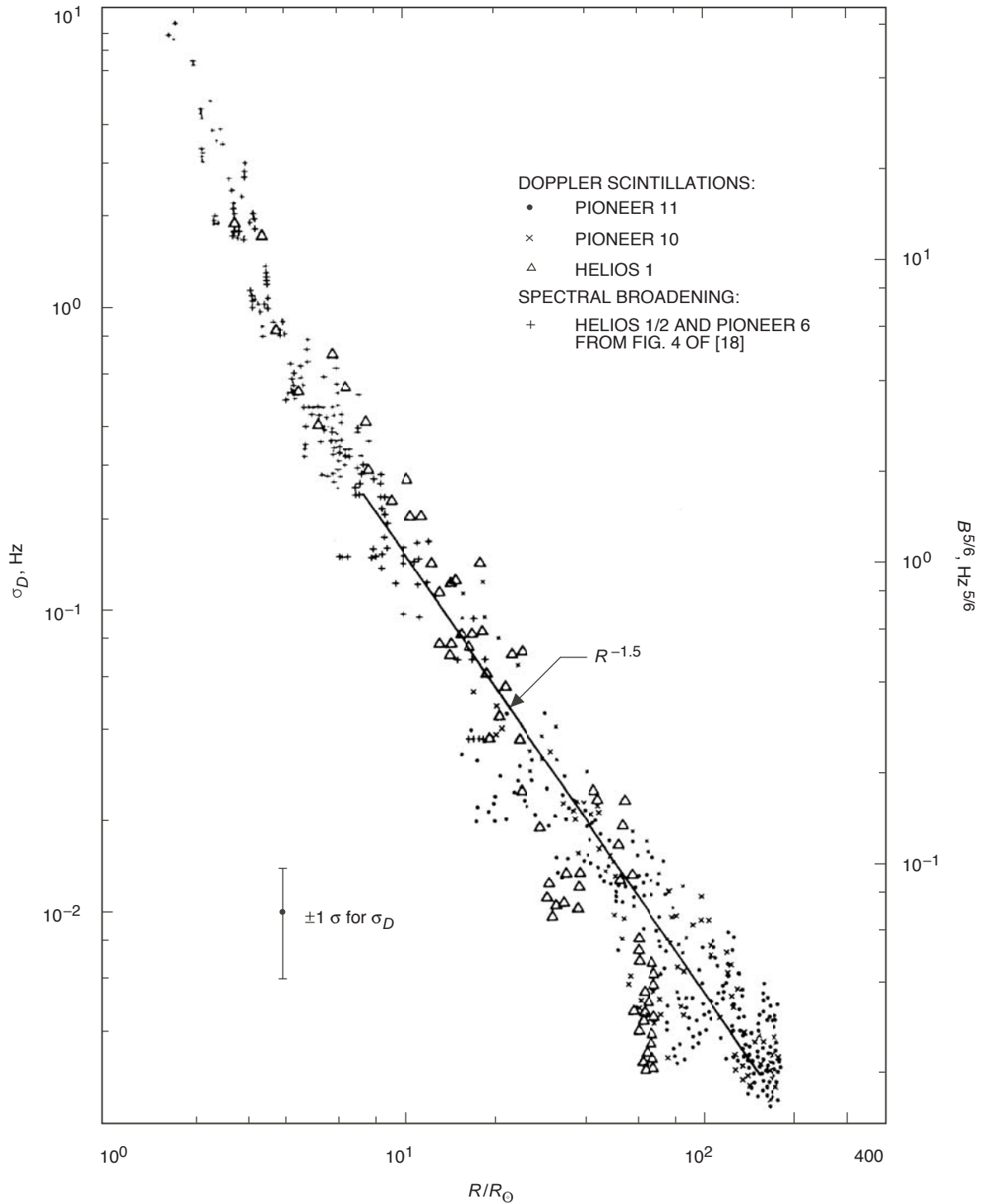
Fig. 2. Systematic increase toward the Sun of spectral broadening characterized by band-width B of the S-band (2.3 GHz, 13 cm) radio signal and Doppler scintillation characterized by its rms σ_D (adapted from Fig. 11 of [18]). Beyond about 10 R_o ($\varepsilon = 2.7$ deg), the radial dependence follows $R^{-1.5}$, corresponding to a radial dependence of R^{-2} for the density fluctuations. Since the solar wind expands radially, this suggests that the solar wind acceleration is essentially over. Near the Sun, the steeper radial dependence is a manifestation of the acceleration of the solar wind.
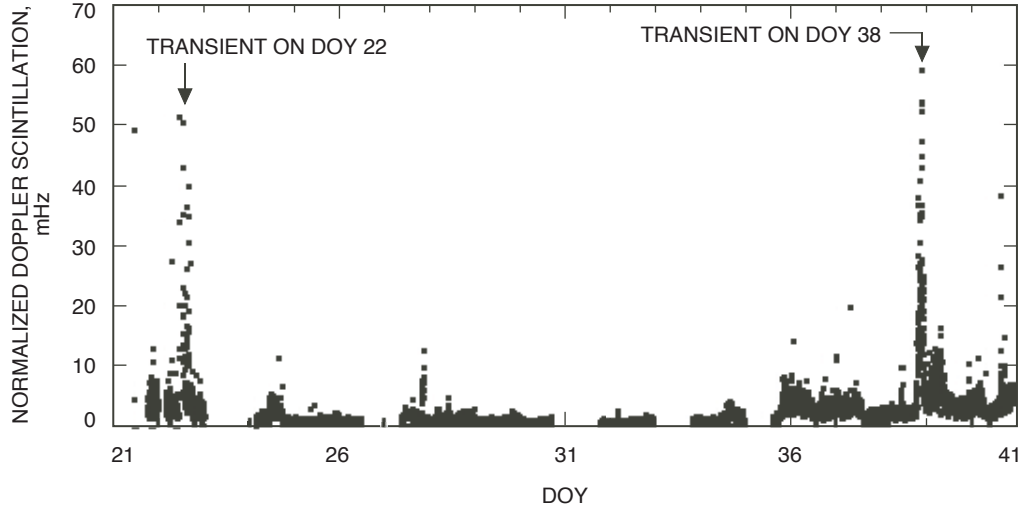
Fig. 3. Time series of Galileo rms Doppler scintillation observed during 1997. Two prominent transients are detected on DOY 22 (January 22, 1997) when the closest approach point was at 15 R_O **or** ε = 4 deg**, and the other on DOY 38 (February 7, 1997) when it was at** 55 R_O **or** ε = 14.8 deg**.**

pronounced enhancement in scintillation are immediately apparent, with the one on February 7, 1997, day of year (DOY) 38, being responsible for the disruption in Galileo communications mentioned earlier. It corresponds to the CME imaged by the SOHO Large Angle Spectrometric Coronagraph (LASCO) moving off the west limb of the Sun about 20 hours earlier, and it is described as a halo event [28]. Figure 4 shows the expanded Doppler scintillation time series, the time-lapse LASCO images, and the height–time diagram of the CME. The enhanced scintillation at the leading edge of the transient is typical of coronal mass ejections and represents the compressed plasma ahead of the apparent shock. The scintillation remains disturbed for a couple of days, which is also typical of the passage of CMEs. The large fields of view of the LASCO coronagraphs make them particularly well suited for imaging CMEs. That LASCO monitors the corona continuously makes it invaluable not only for diagnosing radio-propagation problems but, as illustrated in the height–time diagram of Fig. 3, also for forecasting them. In this particular case, a 20-hour advance warning could in principle have been issued to the Galileo Project.

Synoptic studies have shown that during the period from 1978 to 1988 Doppler scintillation transients occurred at a rate of approximately once every 4.6 days near solar minimum and once every 13 days during solar maximum. This 11-year solar cycle transient-rate variation is similar to that of the CME rate deduced from coronagraph observations, hence showing that many of the Doppler scintillation transients represent CMEs. The impact of a CME can be characterized by its strength, as described by the ratio of its peak-to-pre-transient or background scintillation level, called the enhancement factor (EF). While EF tended to diminish with increasing heliocentric distance or solar elongation during high solar activity, it was more evenly distributed during low solar activity. EF also was lower during solar minimum, as 13 percent of the transients during solar maximum had values exceeding 23, the highest EF observed during solar minimum. These results are consistent with the fact that occasional major fast-moving interplanetary shocks observed during solar maximum (see, e.g., [30]) seem rare during solar minimum. More information on CMEs and their properties relevant to radio effects has become available from the highly successful white-light observations of SOHO LASCO[5] [36].

---

[5] http://lasco-www.nrl.navy.mil/index.php

(a)

(b)

C2 1997/02/07 01:30:05   C2 1997/02/07 02:30:05   C2 1997/02/07 03:30:05

(c)

○ LASCO WHITE LIGHT
● GALILEO DOPPLER SCINTILLATION
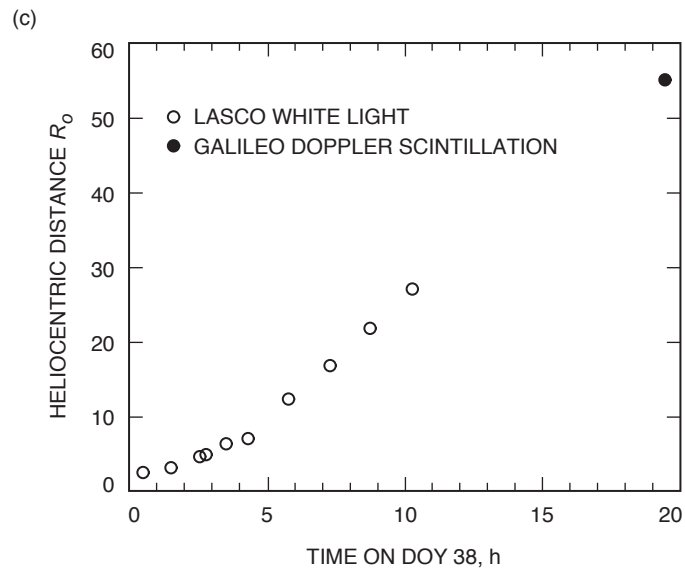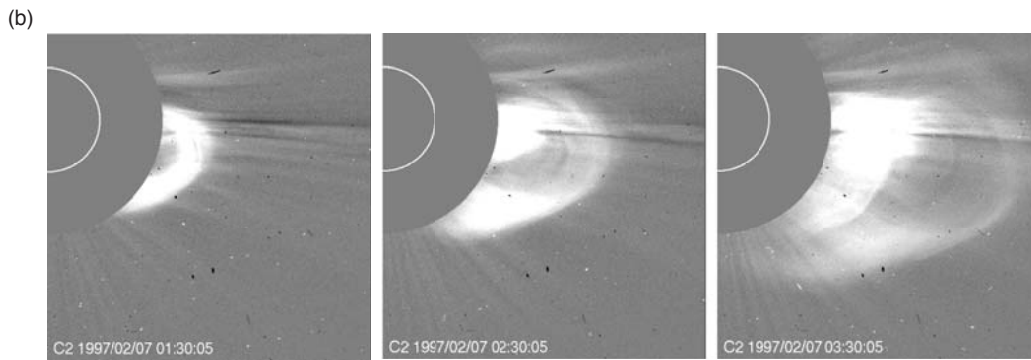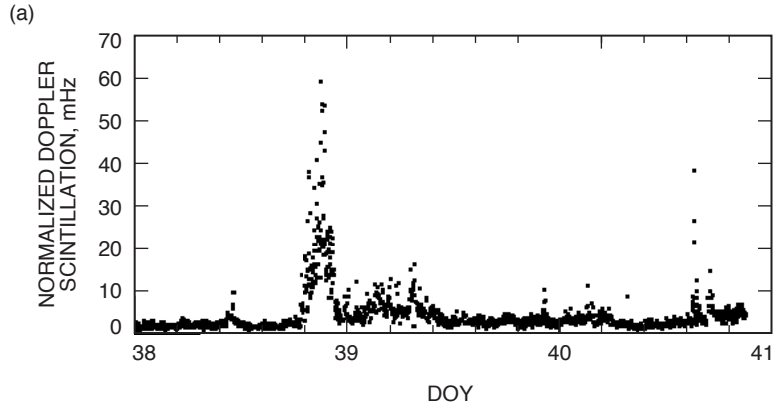
Fig. 4. Observations of the coronal mass ejection of February 7, 1997 (DOY 38): (a) expanded time series of the Galileo Doppler scintillation measurements, showing the DOY 38 transient of Fig. 3, (b) corresponding coronal mass ejection CME seen by SOHO LASCO 20 hours earlier, and (c) height–time diagram of CME, showing the detection of the LASCO CME by the Galileo Doppler scintillation measurements at a radial distance of $55\ R_o$**.**

IV. Heliospheric Current Sheet

As with in situ point measurements of the solar wind, the bane of radio occultation measurements is their inability to distinguish spatial from temporal variations using only the data themselves. Thus, while propagating disturbances like CMEs are an obvious cause of Doppler scintillation transients, co-rotating quasi-stationary structures that are anchored at, and rotate with, the Sun across the radio path are not. For this reason, the spatial or longitudinal organization of enhanced small-scale density fluctuations in general [37], and the signature of the heliospheric current sheet in particular [38], eluded radio occultation investigations of the solar corona and solar wind for a long time. The heliospheric current sheet is the magnetic boundary encircling the Sun that separates oppositely directed solar magnetic fields [39]. The magnetic polarity reversal of the current sheet [40] is embedded in a thin sheet of enhanced plasma and enhanced density fluctuations [41]. When the current sheet is transverse to the plane of the sky, i.e., when it is seen edge-on, it appears in white-light images of the corona as the narrow stalk of a streamer [11]. Farther from the Sun, in the solar wind probed directly by interplanetary spacecraft, the counterpart of the streamer stalk is the heliospheric plasma sheet, which is characterized by a narrow region of enhanced density and density fluctuations surrounding the magnetic polarity reversal [35, 42–44].

The other Doppler scintillation transient in Fig. 3 observed on January 22, 1997 (DOY 22), represents the heliospheric current sheet observed edge-on when it crosses the Galileo radio path, as confirmed by the streamer stalk in the LASCO image of Fig. 5. The expanded time series shows that the enhanced scintillation, representing the presence of filamentary structures with enhanced transverse density gradients, lasts a few hours, typical for streamer stalk crossings and reflecting the narrowness of the streamer stalks [41]. Since a stalk moves across the plane of the sky as it rotates with the Sun at an approximate rotation rate of 27 days [46], the LASCO images again can serve to identify and predict when the stalks might traverse a radio path.

V. Active Regions

The temporal/spatial ambiguity that masked the signature of the heliospheric current sheet also plagued a fuller understanding of the nature of the small-scale density fluctuations observed by radio occultation measurements. Long thought to represent mainly small-scale turbulence or random electron density inhomogeneities that are convected along with the solar wind [19], the corona is in fact also pervaded by predominantly radial filamentary structures extending from, and rotating with, the Sun [47]. These filamentary structures span a wide range of scale sizes, the smallest having a transverse scale of a kilometer at the Sun, more than two orders of magnitude finer than the smallest structures seen in coronal images [47,48].

Figure 6 shows composite images of the August 11, 1999, solar eclipse based on ground-based and SOHO LASCO C2 images of path-integrated density produced by Koutchmy et al. [49]. The processed picture, which shows an abundance of filamentary structures, was obtained through application of an algorithm to the eclipse picture that detects and follows structures characterized by enhanced gradients [50], a process referred to as edge enhancement. The unprocessed image is of the same path-integrated density structure that is observed by radio ranging measurements, while the processed pictures reveal the small-scale density structures detected by Doppler measurements [7,8]. Multiple-station intensity-scintillation measurements [51,52] and time-lapse white-light measurements [53] show that inhomogeneities or turbulence convected along with the solar wind are also present in the corona. However, filamentary structures dominate the processed image of Fig. 6 for the same reason that they dominate Doppler scintillation measurements. The transverse density gradients of the filamentary structures are significantly steeper than those of the convected turbulence [8,47].

While predominantly radial filamentary structures emanate everywhere from the Sun and permeate the entire corona, those associated with active regions where the magnetic fields are strong and complex have significantly enhanced transverse density gradients [7,8]. Thus, when an active region rotates at

(a)

(b)
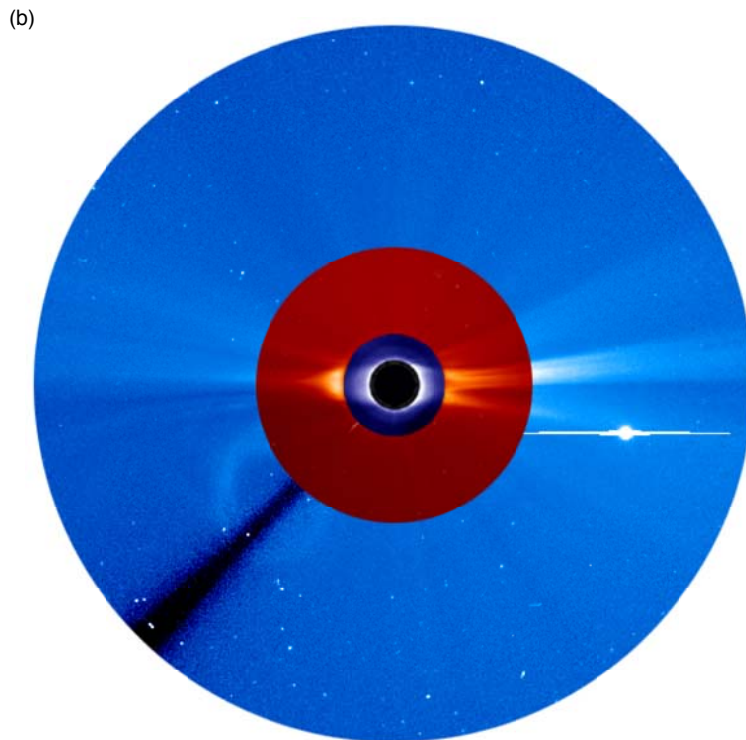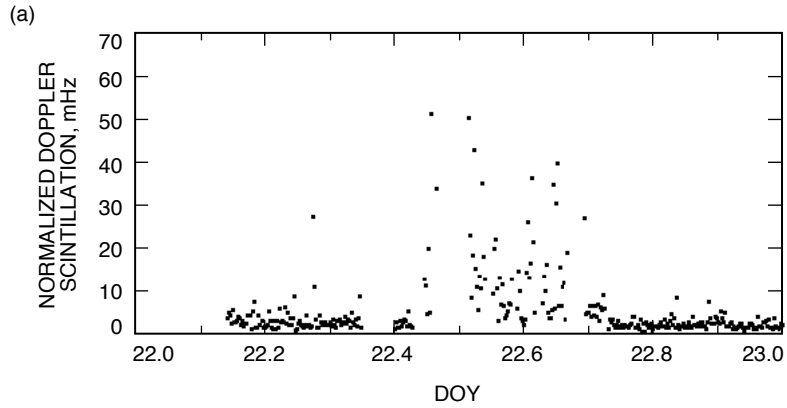
Fig. 5. Observations of the streamer stalk of February 22, 1997 (DOY 22): (a) expanded time series of the Galileo Doppler scintillation measurements, showing the DOY 22 transient of Fig. 3 and (b) composite High Altitude Observatory Mauna Loa Mk III [45] and SOHO LASCO C2 and C3 white-light coronagraph images. The large white dot corresponds to Jupiter, around which the Galileo spacecraft was orbiting. The intersection of Jupiter and the narrow streamer stalk indicates that the observed Galileo Doppler scintillation is a result of the intersection of the Galileo radio path and the streamer stalk representing the heliospheric current sheet observed edge-on.

8
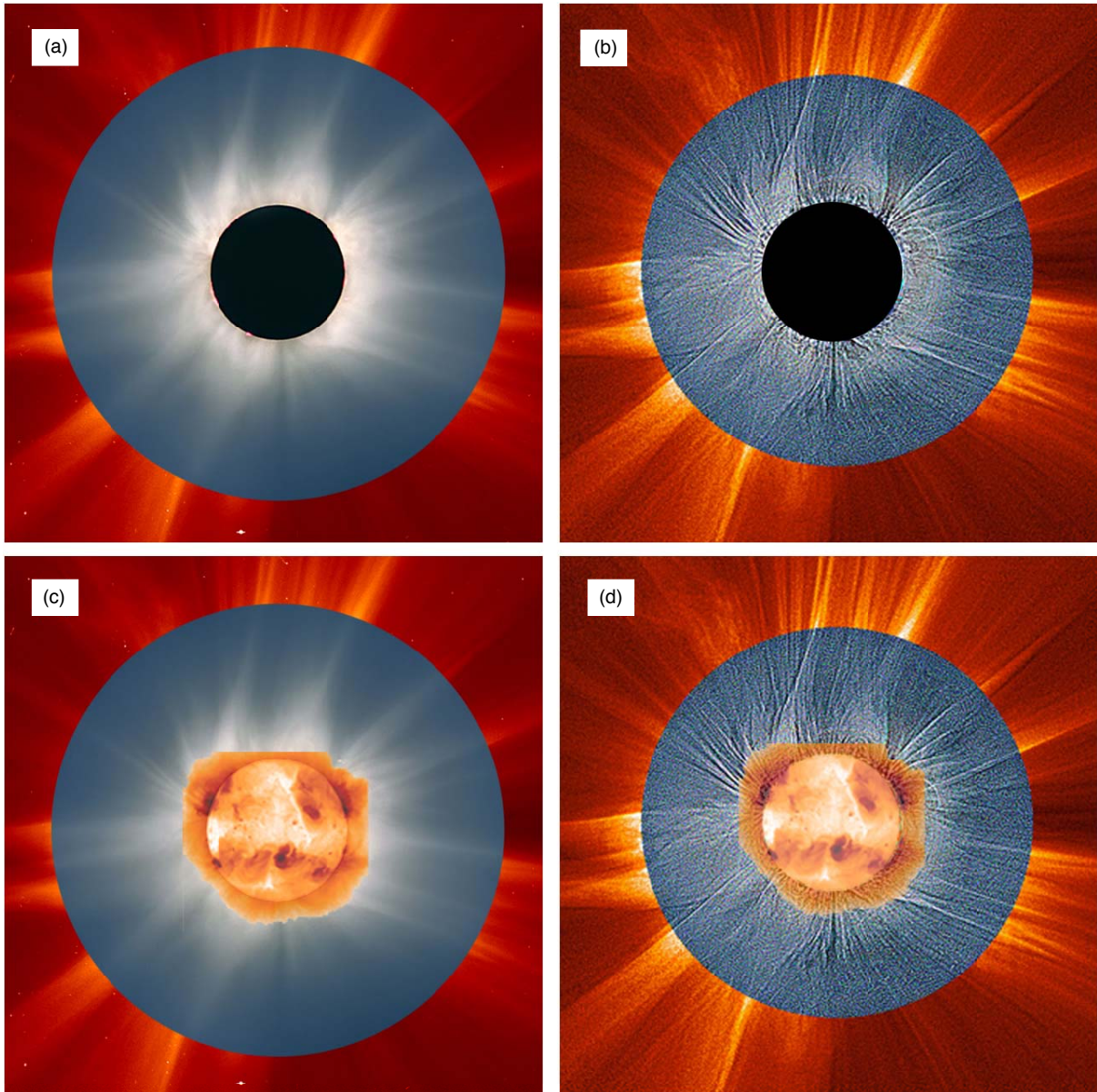
Fig. 6. White-light images of the August 11, 1999, solar eclipse: (a) combined eclipse and SOHO LASCO C2 white-light images of the August 11, 1999, solar eclipse with north pointing up [49]; occurring during solar maximum, the corona shows streamers at all latitudes, and (b) edge-enhanced image revealing filamentary structures at the image resolution of 1 deg in latitude [49]. In addition to the low-lying closed loops, striking open filamentary structures emanate from the entire Sun. The Yohkoh image of the solar disk is superimposed on the images of (a) and (b) and shown in (c) and (d), respectively. The open filamentary structures associated with the active regions on the northeast and northwest limb are especially pronounced because their transverse density gradients are steepest [8].

the limb of the Sun, the strong filamentary structures extending from it (see evidence for some of the larger filamentary structures in the processed image of Fig. 6) cause enhanced scintillation to an overlying radio path. This is illustrated in the Ulysses ranging and Doppler measurements made during DOYs 54 through 74 (February 23 through March 15) in 1995 [54] and reproduced in Fig. 7. As revealed in Fig. 7(b), enhanced scintillation was observed during the period of DOYs 64 through 68 (March 5 through 9), and from the sequence of daily Yohkoh images of soft x-ray emission shown in Fig. 8, it is clear that the disturbed period of enhanced scintillation corresponds to the passage of a cluster of active regions
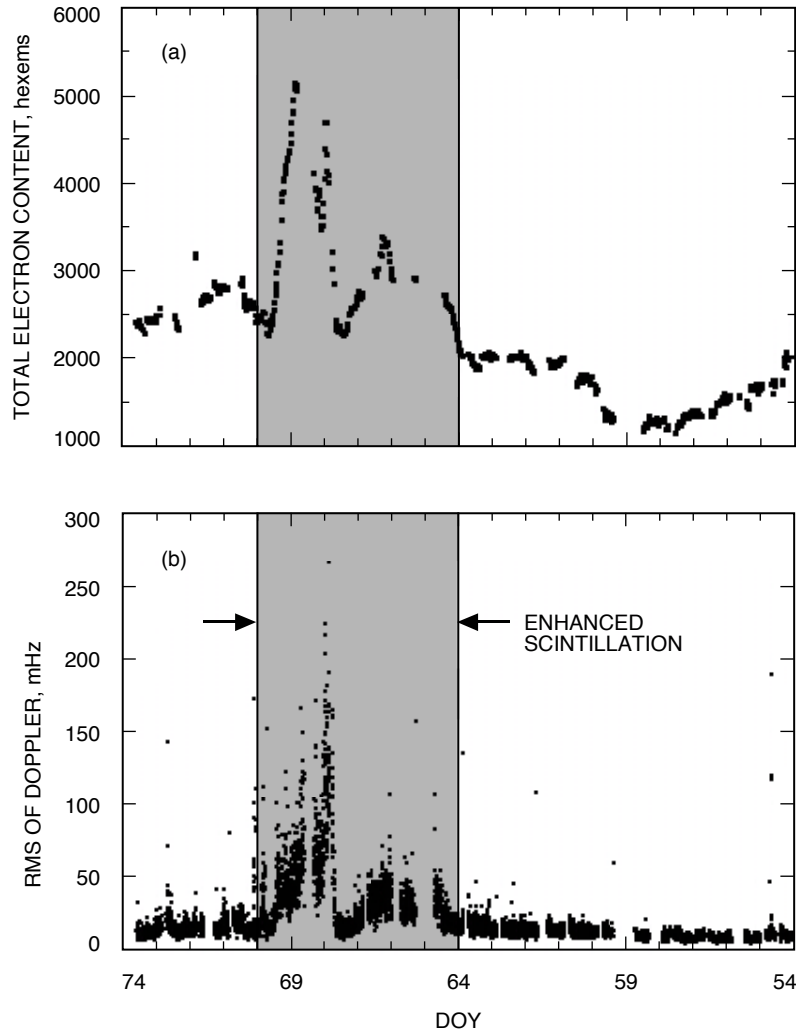
Fig. 7. Time histories of (a) 30-minute ranging measurements in hexems (10^{16} electrons/m^2) observed by Ulysses during DOYs 54 through 74 (February 23 through March 15) in 1995 and normalized to 25 R_O [54], and (b) 3-minute Doppler scintillation observed by Ulysses during 1995 and normalized to 25 R_O [54]. Note that Doppler scintillation is enhanced during DOYs 64 through 68 (March 5 through 9).

underneath the Ulysses radio path. The enhanced scintillation is caused by the crossing of the Ulysses radio path by predominantly radial filamentary structures associated with, and emanating from, the active regions below, and characterized by strong transverse density gradients.

Although soft X-ray observations are no longer available from Yohkoh, the recently launched Hinode (Solar B)[6] spacecraft soon will provide them at even higher resolution. Furthermore, long-lived active regions are also observed by the SOHO Extreme Ultraviolet Imaging Telescope) (EIT).[7] This routine imaging of active regions is, therefore, also useful for diagnosing and forecasting space weather.

---

[6] http://hinode.nao.ac.jp/index_e.shtml

[7] http://umbra.nascom.nasa.gov/eit/

(a)

10$R_\odot$ 20   30   75 40   50
                                              ecliptic
77
73
71
69
67
65
63
61
59
2000
57
3000
55
53
51 4000 hexems

(b)   DOY 62   DOY 63   DOY 64

DOY 65   DOY 66   DOY 67

DOY 68   DOY 69   DOY 70
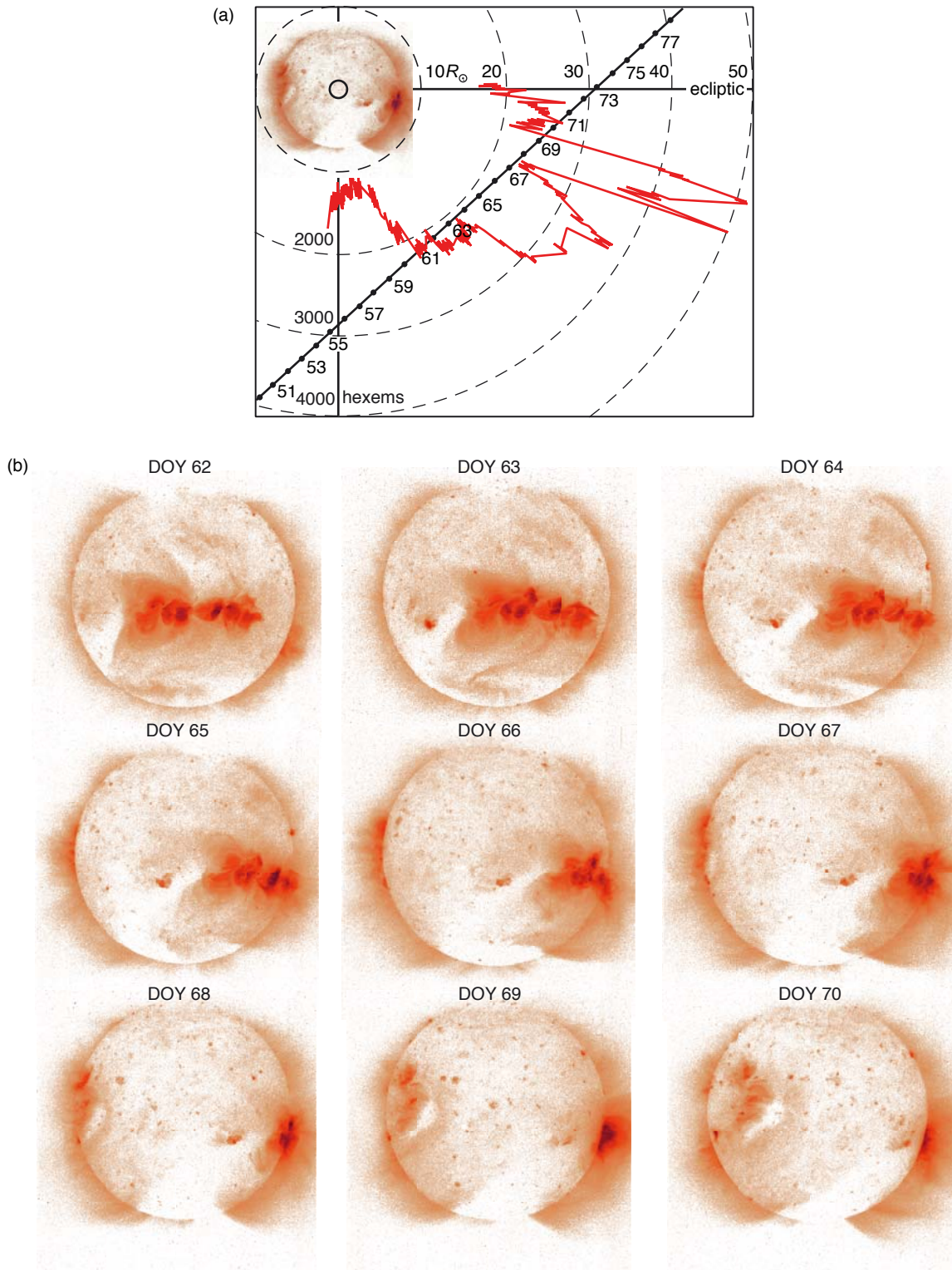
Fig. 8. Ulysses radio path relative to the Sun: (a) the Ulysses radio path as it moves across the plane of the sky from high to low latitude during the time of ranging and Doppler scintillation measurements shown in Fig. 7; the red curve represents the polar plot of ranging in Fig. 7, and (b) daily Yohkoh soft x-ray images reveal that the period of enhanced Doppler scintillation shown in Fig. 7(b) corresponds to the rotation of a cluster of active regions underneath the Ulysses radio path.

11

VI. Conclusions

We have described here how coronal mass ejections, the heliospheric current sheet, and active regions give rise to enhanced small-scale density fluctuations, and hence represent adverse space weather to deep-space communications. We have illustrated how daily observations of the Sun made possible by unprecedented solar missions like SOHO and Yohkoh can play an important role in diagnosing, monitoring, and forecasting such space-weather effects. These practical benefits are the culmination of five decades of probing the solar corona with radio occultation measurements. That it has taken this long is a testament to the challenging nature of the problem, which required wide-ranging investigations. In addition to carrying out a large number of radio experiments, and acquiring and processing the data, these have included

- Performing theoretical studies of wave propagation through the solar corona in order to understand the diverse radio phenomena and extract plasma properties from them

- Exploring and characterizing the plasma properties deduced from the diverse radio measurements and unifying them into a coherent picture of global distribution

- Determining the nature of the electron density variations from their inferred properties in the face of spatial-temporal ambiguity

- Relating the global density variations from radio measurements to, and integrating them with, disparate global observations of the Sun, corona, and solar wind

Acknowledgments

References

[1] R. M. Goldstein, "Superior Conjunction of Pioneer 6," *Science*, vol. 166, pp. 598–601, 1969.

[2] G. S. Levy, T. Sato, B. L. Seidel, C. T. Stelzried, J. E. Ohlson, and W. V. T. Rusch, "Pioneer 6: Measurement of Transient Faraday Rotation Phenomena Observed during Solar Occultation, *Science*, vol. 166, pp. 596–598, 1969.

[3] J. W. Dyer, "Pioneer Saturn," *Science*, vol. 207, pp. 400–401, 1980.

[4] K. E. Machin and F. G. Smith, "Occultation of a Radio Star by the Solar Corona," *Nature*, vol. 170, pp. 319–320, 1952.

[5] A. Hewish, "The Irregular Structure of the Outer Regions of the Solar Corona," *Proc. Roy. Soc., A*, vol. 228, pp. 238–251, 1955.

[6] V. V. Vitkevich, *Dokl. Akad. Nauk. U.S.S.R.*, vol. 101, p. 429, 1955.

[7] R. Woo, "Ultra-Fine-Scale Filamentary Structures in the Outer Corona and the Solar Magnetic Field," *Astrophysical Journal*, vol. 639, pp. L95–L98, 2006.

[8] R. Woo, "Filamentary Structures of Solar Eclipse White-Light Images," *Solar Phys.*, submitted 2006.

[9] R. Woo, S. R. Habbal, and U. Feldman, "Role of Closed Magnetic Fields in Solar Wind Flow, *Astrophysical Journal*, vol. 612, pp. 1171–1174, 2004.

[10] R. Woo, "Relating White-Light Coronal Images to Magnetic Fields and Plasma Flow," *Solar Phys.*, vol. 231, pp. 71–85, 2005.

[11] R. Woo and S. R. Habbal, "Origin and Acceleration of the Slow Solar Wind," *Astrophysical Journal*, vol. 629, pp. L129–L132, 2005.

[12] R. Woo, F.-C. Yang, and A. Ishimaru, "Structure of Density Fluctuations Near the Sun Deduced from Pioneer-6 Spectral Broadening Measurements," *Astrophysical Journal*, vol. 210, pp. 593–602, 1976.

[13] A. Hewish, P. F. Scott, and D. Wills, "Interplanetary Scintillation of Small Diameter Radio Sources," *Nature*, vol. 203, pp. 1214–1217, 1964.

[14] P. S. Callahan, "Interpretation of Columnar Content Measurements of the Solar-Wind Turbulence," *Astrophysical Journal*, vol. 187, pp. 185–190, 1974.

[15] R. Woo, "Multifrequency Techniques for Studying Interplanetary Scintillations," *Astrophysical Journal*, vol. 201, pp. 238–248, 1975.

[16] P. S. Callahan, "Columnar Content Measurements of the Solar-Wind Turbulence Near the Sun," *Astrophysical Journal*, vol. 199, pp. 227–236, 1975.

[17] R. Woo, F.-C. Yang, and K. W. Yip, "Measurements of Large-Scale Density Fluctuations in the Solar Wind Using Dual-Frequency Phase Scintillations," *Astrophysical Journal*, vol. 210, pp. 568–574, 1976.

[18] R. Woo, "Radial Dependence of Solar Wind Properties Deduced from Helios 1/2 and Pioneer 10/11 Radio Scattering Observations," *Astrophysical Journal*, vol. 219, pp. 727–739, 1978.

[19] R. Woo and J. W. Armstrong, "Spacecraft Radio Scattering Observations of the Power Spectrum of Electron Density Fluctuations in the Solar Wind," *J. Geophys. Res.-Space Physics*, vol. 84, pp. 7288–7296, 1979.

[20] J. W. Armstrong, "Low-Frequency Gravitational Wave Searches Using Spacecraft Doppler Tracking," *Living Reviews in Relativity*, vol. 9, 2006, 1 (online article), accessed January 31, 2006, http://www.livingreviews.org/lrr-2006-1.

[21] W. A. Coles, "Interplanetary Scintillation," *Space Sci. Rev.*, vol. 21, pp. 411–425, 1978.

[22] J. W. Armstrong and R. Woo, "Solar Wind Motion within 30 R_o: Spacecraft Radio Scintillation Observations," *Astron. Astrophys.*, vol. 103, pp. 415–421, 1981.

[23] R. Woo, "A Synoptic Study of Doppler Scintillation Transients in the Solar Wind," *J. Geophys. Res.-Space Science*, vol. 93, pp. 3939–3926, 1988.

[24] R. A. Howard, N. R. Sheeley, Jr., M. J. Koomen, and D. J. Michels, "Coronal Mass Ejections: 1979-1981," *J. Geophys. Res.-Space Science*, vol. 90, pp. 8173–8191, 1985.

[25] A. J. Hundhausen, "Sizes and Locations of Coronal Mass Ejections: SMM Observations from 1980 and 1984-1989," *J. Geophys. Res.-Space Science*, vol. 98, pp. 13,177–13,200, 1993.

[26] N. R. Sheeley, Jr., R. A. Howard, M. J. Koomen, D. J. Michels, R. Schwenn, K.-H. Mulhauser, and H. Rosenbauer, "Coronal Mass Ejections and Interplanetary Shocks," *J. Geophys. Res.-Space Science*, vol. 90, pp. 163–175, 1985.

[27] R. A. Howard, G. E. Brueckner, O. C. S. Cyr, D. A. Biesecker, K. P. Dere, M. J. Koomen, C. M. Korendyke, P. L. Lamy, A. Llebaria, M. V. Bout, D. J. Michels, J. D. Moses, S. E. Paswaters, S. P. Plunkett, R. Schwenn, G. M. Simnett, D. G. Socker, S. J. Tappin, and D. Wang, "Observations of CMEs from SOHO/LASCO," in *Coronal Mass Ejections*, N. Crooker, J. A. Joselyn, and J. Feynman, eds., Geophysical Monograph 99, American Geophysical Union, Washington, D.C., pp. 17–26, 1997.

[28] S. P. Plunkett, N. Gopalswamy, M. R. Kundu, R. A. Howard, B. J. Thompson, J. B. Gurman, R. P. Lepping, H. S. Hudson, N. Nitta, Y. Hanaoka, T. Kosugi, and J. T. Burkepile, "A Multi-Wavelength Analysis of the February 6/7, 1997 Coronal Mass Ejection," *Proc. 5th SOHO Workshop, The Corona and Solar Wind Near Minimum Activity*, Oslo, Norway, June 17–20, 1997, ESA SP-404, September 1997.

[29] H. Morgan, S. R. Habbal, and R. Woo, "The Depiction of Coronal Structure in White-Light Pictures," *Solar Phys.*, vol. 236, pp. 263–272, 2006.

[30] R. Woo and J. W. Armstrong, "Measurements of a Solar Flare-Generated Shock Wave at 13.1 R_o," *Nature*, vol. 292, pp. 608–610, 1981.

[31] R. Woo, J. W. Armstrong, N. R. Sheeley, Jr., R. A. Howard, M. J. Koomen, D. J. Michels, and R. Schwenn, "Doppler Scintillation Observations of Interplanetary Shocks Within 0.3 AU," *J. Geophys. Res.-Space Science*, vol. 90, pp. 154–162, 1985.

[32] R. Woo and R. Schwenn, "Comparison of Doppler Scintillation and In Situ Spacecraft Plasma Measurements of Interplanetary Disturbances," *J. Geophys. Res.-Space Science*, vol. 96, pp. 21,227–21,244, 1991.

[33] R. Woo, J. W. Armstrong, N. R. Sheeley, Jr., R. A. Howard, D. J. Michels, and M. J. Koomen, "Simultaneous Radio Scattering and White Light Observations of a Coronal Transient," *Nature*, vol. 300, pp. 157–159, 1982

[34] R. Woo, "Solar Cycle Variation of Interplanetary Disturbances Observed as Dopppler Scintillation Transients," *J. Geophys. Res.-Space Science*, vol. 98, pp. 18,999–19,004, 1993.

[35] D. E. Huddleston, R. Woo, and M. Neugebauer, "Density Fluctuations in Different Types of Solar Wind Flow at 1 AU and Comparison with Results from Doppler Scintillation Measurements Near the Sun," *J. Geophys. Res.-Space Science*, vol. 100, pp. 19,951–19,956, 1995.

[36] S. Yashiro, N. Gopalswamy, G. Michalek, O. C. St. Cyr, S. P. Plunkett, N. B. Rich, and R. A. Howard, "A Catalog of White Light Coronal Mass Ejections Observed by the SOHO Spacecraft," *J. Geophys. Res.-Space Science*, vol. 109, A07105, doi:10.1029/2003JA010282, 2004.

[37] R. Woo and P. Gazis, "Large-Scale Solar-Wind Structure Near the Sun Detected by Doppler Scintillation," *Nature*, vol. 366 pp. 543–545, 1993.

[38] R. Woo, J. W. Armstrong, and P. R. Gazis, "Doppler Scintillation Measurements of the Heliospheric Current Sheet and Coronal Streamers Close to the Sun," *Space Sci. Rev.*, vol. 72, pp. 223–228, 1995.

[39] E. J. Smith, "The Heliospheric Current Sheet," *J. Geophys. Res.-Space Science*, vol. 106, pp. 15,819–15,831, 2001.

[40] R. Woo, "Evidence for the Reversal of Magnetic Field Polarity in Coronal Streamers," *Geophys. Res. Lett.*, vol. 24, pp. 97–100, 1997.

[41] R. Woo, J. W. Armstrong, M. K. Bird, and M. Pätzold, "Fine-Scale Filamentary Structure in Coronal Streamers," *Astrophysical Journal*, vol. 449, pp. L91–L94, 1995.

[42] J. T. Gosling, G. Borrini, J. R. Asbridge, S. J. Bame, W. C. Feldman, and R. T. Hansen, "Coronal Streamers in the Solar Wind at 1 AU," *J. Geophys. Res.-Space Science*, vol. 86, pp. 5438–5448, 1981.

[43] D. Winterhalter, E. J. Smith, M. E. Burton, N. Murphy, and D. J. McComas, "The Heliospheric Plasma Sheet," *J. Geophys. Res.-Space Science*, vol. 99, pp. 6667–6680, 1994.

[44] B. Bavassano, R. Woo, and R. Bruno, "Heliospheric Plasma Sheet and Coronal Streamers," *Geophys. Res. Lett.*, vol. 24, pp. 1655–1658, 1997.

[45] R. Fisher, R. H. Lee, R. M. MacQueen, and A. I. Poland, "New Mauna Loa Coronagraph Systems," *Appl. Optics*, vol. 20, pp. 1094–1101, 1981.

[46] Y.-M. Wang, N. R. Sheeley, Jr., R. A. Howard, J. R. Kraemer, N. B. Rich, M. D. Andrews, G. E. Brueckner, K. P. Dere, M. J. Koomen, C. M. Korendyke, D. J. Michels, J. D. Moses, S. E. Pasaters, D. G. Socker, D. Wang, P. L. Lamy, A. Llebaria, D. Vibert, R. Schwenn, and G. M. Simnett, "Origin and Evolution of Coronal Streamer Structure During the 1996 Minimum Activity Phase," *Astrophysical Journal*, vol. 485, pp. 875–889, 1997.

[47] R. Woo, "Kilometre-Scale Structures in the Sun's Corona," *Nature*, vol. 379, pp. 321–322, 1996.

[48] R. Woo and S. R. Habbal, "Finest Filamentary Structures of the Corona in the Slow and Fast Solar Wind," *Astrophysical Journal*, vol. 474, pp. L139–L142, 1997.

[49] S. Koutchmy, A. Adjabshirizadeh, F. Baudin, K. Bocchialini, J.-P. Delahoudinière, L. Golub, P. Lamy, and J. Mouette, *Observations et Travaux*, vol. 53, pp. 35–41, 2001.

[50] O. Koutchmy and S. Koutchmy, "Optimum Filter and Frame Integration Application to Granulation Pictures," in *High Spatial Resolution Solar Observations, Proceedings of the 10th Sacramento Peak Summer Workshop*, O. von der Lühe, ed., National Solar Observatory, Sunspot, New Mexico, p. 217, 1989.

[51] A. Hewish, P. A. Dennison, and J. D. H. Pilkington, "Measurements of the Size and Motion of Irregularities in the Interplanetary Medium," *Nature*, vol. 209, pp. 1188–1189, 1966.

[52] R. D. Ekers and L. T. Little, "The Motion of the Solar Wind Close to the Sun," *Astron. Astrophys.*, vol. 10, pp. 310–316, 1971.

[53] N. R. Sheeley, Jr., Y.-M. Wang, S. H. Hawley, G. E. Brueckner, K. P. Dere, R. A. Howard, M. J. Koomen, C. M. Korendyke, D. J. Michels, S. E. Paswaters, D. G. Socker, O. C. St. Cyr, and D. Wang, "Measurements of Flow Speeds in the Corona Between 2 and 30 R_o," *Astrophysical Journal*, vol. 484, pp. 472–478, 1997.

[54] R. Woo and S. R. Habbal, "Extension of Coronal Structure into Interplanetary Space," *Geophys. Res. Lett.*, vol. 24, pp. 1159–1162, 1997.